

# Optical Properties of South Pole Ice at Depths from 140 to 2300 Meters

Kurt Woschnagg<sup>1</sup>, for the AMANDA Collaboration\*

<sup>1</sup>Department of Physics, University of California, Berkeley, CA 94720, USA

## Abstract

Depth and wavelength dependence of absorption and scattering coefficients at the South Pole AMANDA site were mapped with pulsed and D.C. light sources. The contribution of air bubbles to scattering decreases with depth and disappears at  $\sim 1.4$  km; at greater depths scattering by dust dominates. Peaks in scattering at several well-defined depths are attributed to peaks in dust concentration and are consistent with peaks in muon attenuation with depth. The magnitudes of the scattering and absorption are roughly consistent with predictions of the He-Price theory. At depths 1.4 to 2.3 km the optical properties of the ice are suitable for a 1-km<sup>3</sup> high-energy neutrino observatory, except for a 100-m thick dust band at 2.1 km.

## 1 Introduction

Radar mapping studies show that isochrons rarely have slopes greater than 100 m per km, except within a few hundred meters of bedrock. Thus, for a neutrino observatory  $\sim 1$  km on a side, the depths of strong scattering and absorbing layers are nearly horizontal, and ice properties can be characterized with measurements only along a single line in the vertical dimension. Our theoretical work (AMANDA Collaboration, 1997; Price & Bergström, 1997; He & Price, 1998) and experimental papers (Askebjerg et al., 1995, 1997) laid the groundwork for interpretation of the depth- and wavelength-dependent scattering and absorption of light in South Pole ice.

The optical properties were measured *in situ* at various wavelengths with pulsed and D.C. light sources buried at different locations in the ice, and with a powerful dye laser at the surface. The dye laser was used to send nanosecond light pulses at a wavelength of 532 nm through optical fibers down to diffusing balls embedded in the ice near each optical module in the array. For each data run a separate ball location was used, thus enabling us to determine the ice properties over the full AMANDA depth range. In the following, the optical properties are discussed in terms of  $a$  = absorption coefficient,  $b$  = scattering coefficient, and  $b_e = b(1 - \langle \cos \theta \rangle)$  = effective scattering coefficient, where  $\theta$  is the scattering angle.

## 2 Methods of analysis

The pulsed sources were used to measure scattering and absorption independently. The arrival times of light pulses were recorded at optical modules at distances up to 200 m from the source. From the photon arrival time distributions thus obtained, the optical properties were extracted by fits to Monte Carlo data. A large data base of simulated time distributions was first generated for a wide range of optical parameters, using a Monte Carlo method, based on a Mie scattering model, to describe the propagation of photons in the ice. Known systematic detector effects, such as the angular acceptance function of the optical modules, were incorporated into the simulation. The measured arrival time distributions were then compared to Monte Carlo distributions at a grid of discrete points in the parameter space of  $\lambda_a \equiv 1/a$  and  $\lambda_e \equiv 1/b_e$ . This resulted in a  $\chi^2$  surface which was fitted near its minimum with an elliptic paraboloid function, using as six free parameters  $\lambda_a$ ,  $\lambda_e$ , and  $\chi^2_{\min}$  for the location of the minimum, and the statistical errors  $\sigma_a$ ,  $\sigma_e$ , and correlation  $\rho$  for the shape of the  $1\sigma$  contour.

The D.C. light sources were used to determine the propagation length  $\lambda_{\text{prop}} = \sqrt{\lambda_a \lambda_e / 3}$  by measuring the photon flux as a function of distance  $D$  from the source, which is described by a function of the form  $D^{-1} \exp(-D/\lambda_{\text{prop}})$ . Using values for scattering, which depends only weakly on wavelength, from measurements with pulsed sources, the absorption coefficient was then extracted.

---

\*see talk of F.Halzen (HE.6.3.01) for the full author list.

### 3 Scattering and absorption as function of wavelength

Figure 1 shows data on wavelength dependence of scattering and absorption, averaged over depths between  $\sim 1550$  and  $\sim 1900$  m. The curves are theoretical predictions calculated by He and Price (1998). They used the three-component model of absorption (AMANDA Collaboration, 1997), which assumes that  $a(\lambda) = 8 \times 10^{39} e^{-0.48\lambda} + 8100 e^{-6700/\lambda} + CM_{\text{dust}} \lambda^{-\kappa}$ . The two exponentials, fitted to laboratory data shortward of 190 nm and longward of 600 nm, account for absorption by pure ice in the absence of dust. The third term, approximated here by a power law with  $\kappa \approx 1$ , gives the contribution of dust, which dominates at wavelengths between about 200 and 400 nm. In that region the ice does not absorb; its only role is to reduce the refractive index of the dust by the factor  $1/n_{\text{ice}}$ . At the longest wavelengths in the visible, dust contributes less than does ice itself. At 532 nm, for example, the contribution of ice is modeled to be  $a_{\text{ice}} = 0.0275 \text{ m}^{-1}$ , the contribution of dust is typically  $a_{\text{dust}} \approx 0.009 \text{ m}^{-1}$ , and  $a_{\text{total}} \approx 0.0365 \text{ m}^{-1}$ .

He and Price used Mie theory to calculate the third term, assuming that dust in South Pole ice consists of four constituents – insoluble mineral grains, acid droplets, salt grains, and soot. They adopted the log-normal size distributions reported for Antarctic aerosols of the same four types, scaled their concentrations from measurements as a function of depth in Vostok ice, and used an age vs depth model based on a simple scaling relationship (AMANDA Collaboration, 1995).

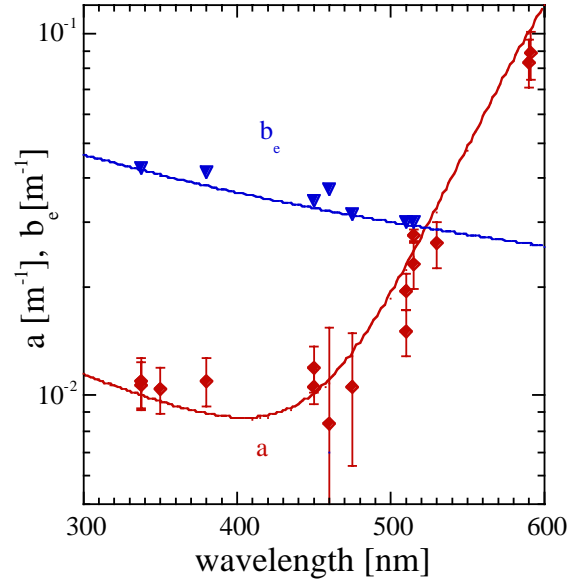


**Figure 1:** Absorption and scattering at average depth of 1.7 km, compared with theory of He and Price (1998).

### 4 Overview of scattering as function of depth throughout South Pole ice

Figure 2 shows  $b(z)$  in four different regimes of depth,  $z$ . At  $z = 140$  to 190 m, Gow (1999) used an optical microscope to measure the size distribution of air bubbles in a shallow core taken at South Pole in 1981.

The dashed curve through his data is calculated for hydrostatic compression of a constant concentration of air bubbles. At depths below 400 m the pressure is sufficiently high that the air bubbles are unstable against a phase transformation into air hydrate crystals, which are transparent and contribute essentially nothing to scattering. The solid curve gives calculated scattering by residual bubbles that have not completed the phase transformation (Price, 1995). At  $z = 800$  to 1000 m, where AMANDA-A is located, the scattering is due almost entirely to bubbles (Askebjerg et al., 1995), with  $b = \int dn(r)/dr \cdot \pi r^2 dr$ , independent of wavelength, and  $r =$  bubble radius. At a depth  $\sim 1300$  m the last air bubbles have transformed into air hydrate crystals. At greater depths scattering is due only to dust. The data at  $z > 1200$  m were taken with the dye laser at 532 nm. Because of forward peaking, effective scattering,  $b_e$ , is smaller by a factor  $\sim 5$  for dust than is geometric scattering,  $b$ .

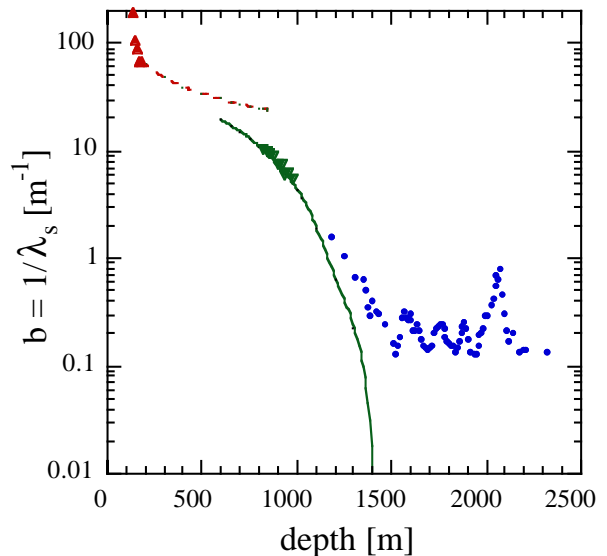


**Figure 2:** Geometric scattering coefficient as a function of depth.

## 5 Scattering and absorption as function of depth at 532 nm

Figure 3 shows our data, together with predictions of the He-Price model, for  $b_e(z)$  and  $a(z)$  at 532 nm. The peaks and valleys in scattering are convincing and show up at the same depths for any cuts on the vertical distance between emitter and receiver,

from a few to a few tens of meters, which indicates that the dust layers extend over several tens of meters, as expected from the predictions in the bottom panel of Fig. 3. At 532 nm absorption is dominated by a constant term due to the ice itself, and the peaks and valleys due to dust are too small to be detectable. At the shorter wavelengths (not yet analyzed), absorption by dust should dominate over absorption by the ice itself, and the peaks and valleys in absorption should show up. The main uncertainty in the He-Price model is the fraction of the acid still in the form of submicron droplets. It is not known to what extent the droplets disperse into crystal boundaries during a residence time in the deep ice of thousands of years. Recent measurements with Raman spectroscopy (Fukazawa et al., 1998) suggest that acids are liquid and mobile only at temperatures above about  $-40^\circ$  C. In Fig. 3, the bottom panel shows predictions based on the assumption that acid does not contribute. The calculated magnitudes of absorption and scattering,  $\sim 0.04 \text{ m}^{-1}$ , agree rather well with average magnitudes of the data. Due to coarseness of binning of the concentrations of the dust components as a function of depth, the peaks and valleys are weak and do not reproduce the strong peaks in the scattering data. Further work is in progress.

The rapid decrease in  $b_e$  at depths  $\sim 1180$  to  $\sim 1400$  m unaccompanied by a rapid decrease in  $a$  is interpreted as due to the decreasing concentration of bubbles, which scatter without absorbing.

## 6 Comparison with results from muon data

AMANDA studies using downgoing atmospheric muons in coincidence with the SPASE array (Tilav, 1998; Miller, 1999) or in coincidence between AMANDA-A and AMANDA-B (Young, 1999) have shown that the probability for Cherenkov photons to hit phototubes is modulated with depth due to variations in dust concentration. Data were obtained for depths  $\sim 1500$  to  $\sim 1900$  m. Maxima in hit probability occur at  $\sim 1680$  and  $\sim 1820$  m and minima at  $\sim 1590$  and  $\sim 1750$  m, with uncertainties of  $\pm 10$  m in depths of maxima and minima. Comparison of the muon data with the 532 nm laser data (Fig. 3) shows that the two results are quite consistent: the depths for maximum muon hit probability correspond to minima in light scattering, and depths for minimum muon hit probability correspond to maxima in scattering.

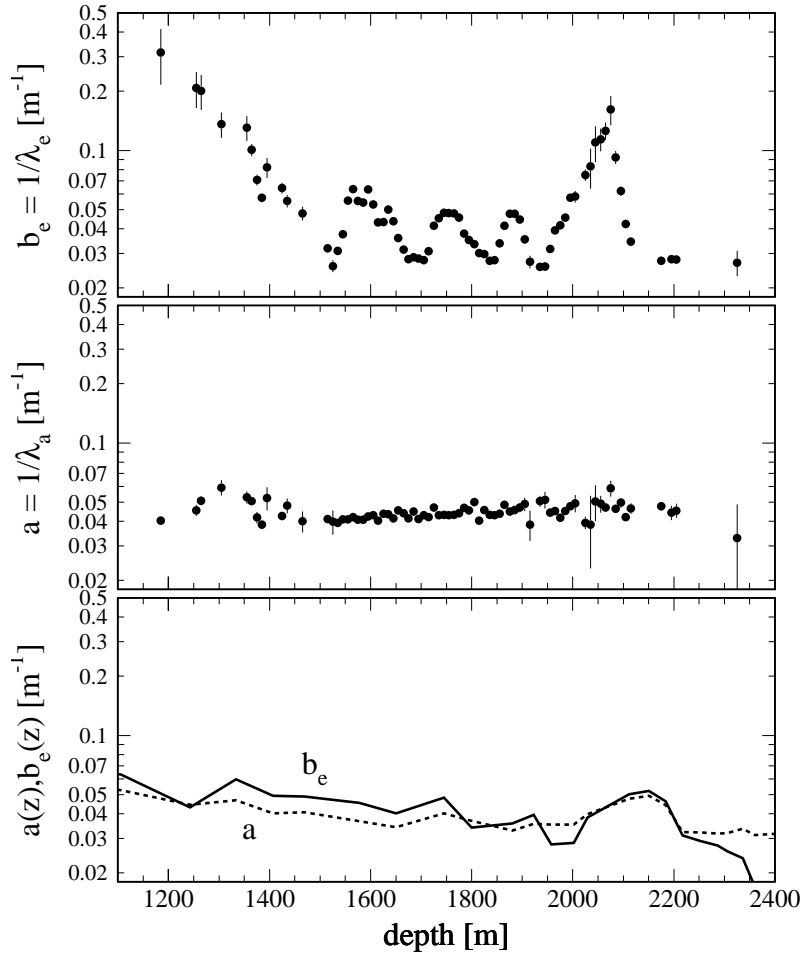


**Figure 3:** Measurements of  $a(z)$  and  $b_e(z)$  at 532 nm, compared with calculations of the He-Price model.

## 7 Conclusions

Our data show that bubbles disappear at a depth of about 1300 to 1400 m, and that at 1.4 to 2.3 km the optical properties of South Pole ice are suitable for a 1-km<sup>3</sup> neutrino observatory, except for a 100-m-thick dust band at 2.1 km.

Minima (maxima) in muon hit probability occur at roughly the same depths as do maxima (minima) in scattering coefficient for 532 nm laser light. The average values of  $a$  and  $b_e$  at 532 nm in the interval  $\sim 1500$  to  $\sim 2300$  m are accounted for reasonably well by the He and Price model (1998), provided acid is assumed to have dispersed into crystal boundaries. Although more work needs to be done in order to make a convincing case, the maxima in scattering and the minima in muon hit probability as a function of depth appear to be correlated with the depths of dust concentrations predicted by He and Price. In order to fit both the absolute magnitude and the peaks and valleys, we plan to adjust the fraction of acid droplets that contribute to scattering and absorption and fine-tune the age vs depth function.

## Acknowledgements

This research was supported by the following agencies: U.S. National Science Foundation, Office of Polar Programs, U.S. National Science Foundation, Physics Division, University of Wisconsin Alumni Research Foundation, U.S. Department of Energy, U.S. National Energy Research Scientific Computing Center (supported by the Office of Energy Research of the U.S. Department of Energy), Swedish Natural Science Research Council, Swedish Polar Research Secretariat, Knut and Alice Wallenberg Foundation, Sweden and the German Ministry of Education and Research.

## References

- AMANDA Collaboration 1995, J. Glaciology 41, 445
- AMANDA Collaboration 1997, Appl. Opt. 36, 4168
- Askebjerg, P., et al. 1995, Science 267, 1147
- Askebjerg, P., et al. 1997, Geophys. Res. Lett. 24, 1355
- Fukazawa, H., et al. 1998, Geophys. Res. Lett. 25, 2845
- Gow, A.J. 1999, private communication
- He, Y.D. & Price, P.B. 1998, J. Geophys. Res. 103, 17041
- Miller, T.C., et al. 1999, these proceedings, HE.6.3.11
- Price, P.B. 1995, Science 267, 1802
- Price, P.B. & Bergström, L. 1997, Appl. Opt. 36, 4181
- Tilav, S. 1998, private communication
- Young, S. 1999, private communication